ELSEVIER

Astroparticle Physics 11 (1999) 457–462

Astroparticle Physics

www.elsevier.nl/locate/astropart

Calibration of a CsI(Tl) crystal with nuclear recoils and pulse shape measurements for dark matter detection

S. Pécourt [a], B. Chambon [a], M. de Jésus [a], D. Drain [a], G. Gerbier [b], J. Mallet [b], M. Massaq [c], L. Mosca [b], C. Pastor [a], C. Tao [d], L. Vagneron [a]

[a] *IPN Lyon, IN2P3-CNRS and Université Claude Bernard Lyon 1, 43 Bd du 11 novembre 1918, F-69622 Villeurbanne Cedex, France*

[b] *DSM/DAPNIA/SPP, C.E. Saclay, F91191 Gif-sur-Yvette, France*

[c] *Université Ibnou Zohr, Agadir, Morroco*

[d] *CPPM, IN2P3/CNRS and Université Aix-Marseille II, 163 ave de Luminy, case 907, F-13288 Marseille Cedex 09, France*

Received 16 November 1998; revised 17 January 1999

Abstract

The quenching factor of cesium and iodine nuclei recoiling in a CsI(Tl) scintillator is measured by scattering of 3 to 6 MeV neutrons. This factor increases when recoil energy decreases, from 7% at 150 keV to 15% at 25 keV. This relatively high efficiency could be useful in experiments dealing with very low recoil energies like the WIMP direct detection. These values are well explained by the Birks model. Pulse shape discrimination between electron and nuclei recoils is also investigated. Results are sufficiently good to allow a significant statistical rejection of radioactive background. This rejection capability is shown to be better than for NaI(Tl), at the same electron equivalent energy.

1. Introduction

The variety of techniques used in direct detection of non-baryonic dark matter demonstrates that there is no universal detector of WIMPs. Different experimental approaches (classic semi-conductor detectors, crystalline or liquid scintillators, bolometers, TPC, superheated superconducting granules) are explored. In spite of their moderate energy resolution, scintillators have an important role to play in this search.

Until now, the choice of NaI [1–5] has been favoured because of its low internal radioactivity, and good scintillation efficiency for Na recoils. Nevertheless, CsI(Tl) has a good luminous efficiency, and measurements reported in this paper show that this scintillator would be a high-performance detector for low energy recoil detection. Of course, a drawback concerning CsI(Tl) is its intrinsic radioactivity (especially ^{137}Cs and ^{134}Cs).

The goal of this paper is twofold: measure the quenching factor of iodine and cesium recoils and analyze the pulse shape differences between nuclear recoils and Compton electron interactions.

2. Experimental procedure

2.1. The method

Incident neutrons produce nuclear recoils in the crystal. At kinetic energies below 6 MeV, neutrons are elastically scattered on Cs nuclei, and both elasti-

0927-6505/99/$ - see front matter
PII S0927-6505(99)00014-6

cally and inelastically on I nuclei. For monoenergetic neutrons, the nucleus recoil energy is determined by measuring the angle of the scattered neutron.

In order to compare the pulse shape of recoil ions and Compton electrons, a ^{137}Cs source was used to induce Compton interactions in the crystal. The high energy of the γ (662 keV) from the ^{137}Cs source allows a uniform spatial distribution of Compton electrons in the CsI(Tl) crystal. This avoids a concentration of low energy surface events, as would be the case with a low energy γ (or X) or β source.

2.2. The setup

The experiment was performed at the 14 MeV Tandem accelerator of the CEN of Bruyères-le-Châtel. The detector is a CsI(Tl) crystal kept at constant room temperature. Its small size (ϕ = 25 mm, h = 25 mm) strongly reduces the fraction of multiple neutron interaction. The crystal is coupled to a RCA 1" photomultiplier with green extended photo-cathode, in order to optimize the photoelectron yield.

The primary proton beam interacts on a tritium target, producing neutrons through the reaction

$$T(p,n)^3He\,.$$

The crystal is positioned at an angle θ = 0° relative to the beam direction and at a distance of 60 cm from the tritium target. Scattered neutrons are detected by five NE213 scintillator detectors (ϕ = 10 cm, h = 5 cm) set in the horizontal plane 120 cm away from the CsI(Tl) crystal, at five angles between 63° and 131° (see Fig. 1) with respect to the beam direction. The pulse shape analysis of the luminous signals in the NE213 detectors allows a discrimination between γ's and neutrons [6]. Each detector is shielded from direct neutrons by paraffin collimators and their solid angle with respect to the CsI(Tl) target is 24.5×10^{-3} steradians. An event is determined by the coincidence between a signal in the CsI(Tl) crystal and a neutron-like signal in one of the NE213 detectors.

For each event, we record

- the time of flight (TOF1) between the HF signal of the beam and the signal of the CsI(Tl) crystal;
- the time of flight (TOF2) between the crystal and the NE213 detectors;
- the NE213 detector light yield;

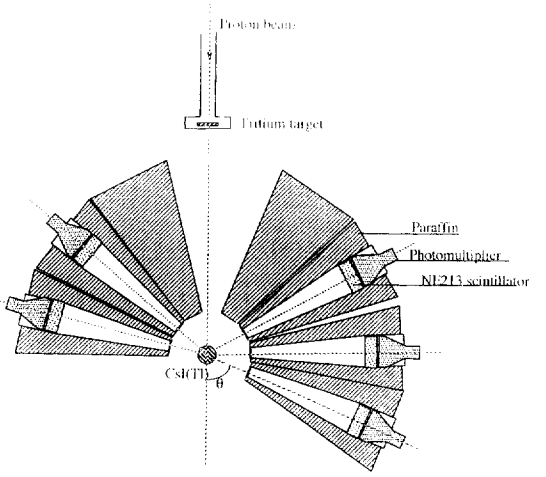

Fig. 1. Experimental setup.

- the neutron-γ PSD information from the NE213 detectors;
- the CsI(Tl) crystal light yield and the time-depending pulse shape.

We reconstruct the TOF between the target and the neutron detectors, to shake off the poor timing of the CsI(Tl) signal.

Elastic events are identified by setting appropriate time-windows on the scatter diagram TF1 vs TOF2.

The scintillation pulse emitted by the CsI(Tl) crystal is digitized at 200 MHz by a Transient Digitizer Lecroy module, in order to analyze the pulse shapes.

3. Quenching factor

Due to the presence of quenching mechanisms, the measured light output from a nuclear recoil L_R of a kinetic energy E is lower than the light output L_{e-} from an electron of the same kinetic energy. The quenching factor α is defined as

$$\alpha = \left.\frac{L_R}{L_{e-}}\right|_E . \qquad (1)$$

Experimentally, α is identical to the ratio of the measured energy of a nuclear recoil using a calibration performed with γ-ray and X-ray sources, E_R^{ee} ("electron equivalent" recoil energy) to the real recoil energy E_R, calculated with the known incident neutron energy and the measured angle of the scattered neutron.

3.1. Result of measurements

The detector was calibrated with a low energy γ source (^{109}Cd) and the response was assumed to be linear in the 4–30 keV energy range. The experimental check of this assumption is reported in Section 3.4.1. The range of recoil energy from 25 keV to 150 keV was explored by varying the incident neutron energy (E_n = 3.0, 3.7, 4.5, 5.3 and 6.0 MeV) and the angle of scattering from 63° to 123°.

Results are reported on Fig. 3. They show an increase of α at low energies.

3.2. Discussion

A recent study of the scintillation efficiency of Ca and F recoils in CaF_2 crystals [7] shows a similar increase of the quenching factor at low energies ($E_0 <$ 1 MeV). On the other hand, it is known that, as large energies, above 1 MeV for heavy ions in alkali halide scintillators for instance [8], the quenching factor increases with energy. This suggests a saturation of scintillation in the energy range where the stopping power is maximum. Indeed, the scintillation efficiency in a CsI(Tl) crystal reverses for alphas around 1 MeV, i.e. at the maximum value of the stopping power [8].

The goal of the next section is to calculate the quenching factor as a function of energy in the energy range of interest here, from known theoretical or empirical descriptions of the stopping power and scintillation efficiency.

3.3. Derivation of light output relations for electrons and recoil ions

The saturation phenomenon in light emission of both inorganic and organic scintillators has been known for a long time [9]. The rate of light produced by an ion per unit of deposited energy dL/dE decreases when the stopping power dE/dx increases. Birks [9] assumed that, for any charged particle, the scintillation efficiency is given by an empirical relation

$$\frac{dL}{dE} = \left(\frac{n_0}{n_{\text{exc}}}\right)\left(\frac{S}{1 + B(dE/dx)}\right), \tag{2}$$

where S is the "absolute scintillation efficiency" and B is an empirical constant. The n_0/n_{exc} ratio with n_0 the initial number of free electrons (or holes) produced in the crystal, and n_{exc} the number of excitons resulting from electron–hole recombination can be written

$$\frac{n_0}{n_{\text{exc}}} = \frac{k(dE/dx)}{1 + k(dE/dx)}, \tag{3}$$

k depending on the crystal compounds.

For electrons, that is, low values of dE/dx, the term n_0/n_{exc} differs noticeably from 1 and should be taken into account, while the term $B(dE/dx)$ becomes negligible.

For high values of dE/dx the n_0/n_{exc} ratio is equal to 1, and the term $B(dE/dx)$ should be taken into account. In addition, the above expression supposes that almost all the particle energy is lost in ionization (electron–hole pairs creation). This is true for high energies, but for lower energies corresponding to stopping power DE/dx below the Bragg maximum, the energy loss by atomic collisions becomes important and this is no longer true. If $\eta(E)$ represents the energy given to electrons, dE/dx in relation (2) should be replaced by the following term:

$$d\eta/dx = \frac{d\eta}{dE} \cdot \frac{dE}{dx}. \tag{4}$$

The dE/dx and $d\eta/dx$ terms are tabulated in the TRIM program [10]. The nuclear energy loss part is based on the Lindhard model [11]. Then integrating relation (2) in both cases of electrons and nuclear recoils, we get the luminous response L_{e-} and L_R. For a given energy E, the term S disappears in the calculation of the ratio α which then depends only on k and B.

3.4. Results of the calculations

3.4.1. Comparison of data to the prediction for L_{e-}

In order to test the L_{e-} calculation and in particular the linearity of the response, we have measured the response of our crystal with standard sources (^{241}Am, ^{57}Co, ^{137}Cs, ^{55}Fe) and X fluorescence of different materials (Cu, Nb, Ag, Ge). The 5 to 60 keV energy range was covered. Results shown on Fig. 2 exhibit the same behaviour as in [8]. After taking into account the correction to get the electron response from the γ response, we can observe nonlinearities of ±8%. The calculation of L_{e-}, based on the integration of Eq. (3), with a standard value of k = 2

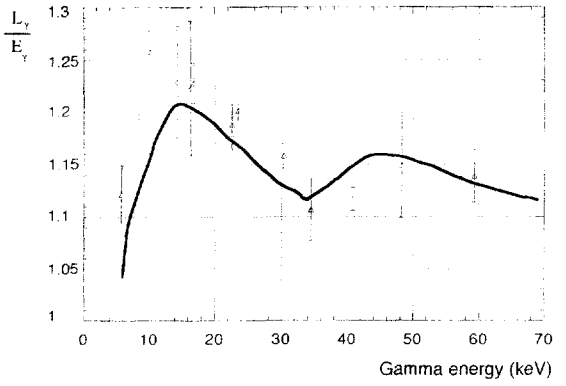

Fig. 2. Luminous experimental response to the "gamma's", normalized to one at 660 keV. The curve is obtained by taking into account the relation between the light response of the crystal to the "gamma's" and the response to the corresponding electrons.

$(\mathrm{keV/mg/cm^2})^{-1}$ predicts at most ±2%. The above assumption of linearity is then valid within 10%.

3.4.2. Comparison of measurements to the prediction for α

The luminous response from ion recoils L_R is obtained as well by integrating Eq. (2) taking into account the relation (4).

So the quenching factor α can be calculated as a function of a single parameter B. From the last section, it is legitimate to compare, within a systematic error of 10%, the calculated α to the experimentally determined value where the linearity of the response in the 4–30 keV range was assumed. This is shown on Fig. 3 where the experimental results are fitted with $B = 14\ (\mathrm{MeV/(mg/cm^2)})^{-1}$.

It is remarkable that both amplitude and variation with energy of the quenching factor are well reproduced by the Birks–Lindhard model, with a single free parameter. The B value found above is within the range of values found at higher energies in CsI(Tl) [12] and other materials and higher energies in CaF_2 [13]). This model is currently tested for low energy data in CaF_2 and NaI(Tl) and is found to be very successful with similar value of B [14]. One could expect a threshold effect to be present at such low energies. A fast decrease of ionization should take place when the energy transferred to an electron becomes lower than the crystal gap energy. This corresponds to a kinetic energy of the Cs and I ions of about 40 keV, a value within the range of energies studied here. Such

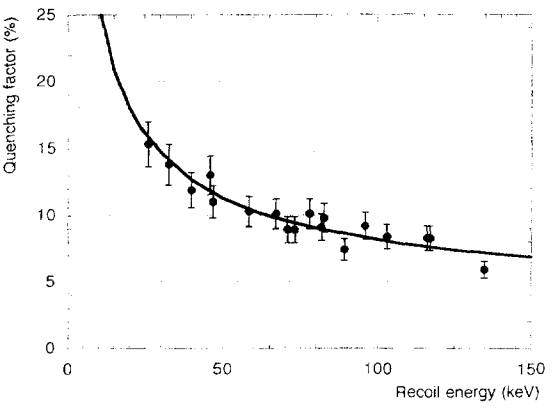

Fig. 3. Experimental quenching factor and calculated one.

effect has indeed already been observed by Ficenec et al. [15] in organic scintillators. However, given the good agreement found above, this effect is small for the CsI(Tl) scintillator.

4. Pulse shape discrimination

With its well-known discrimination capability between electrons and highly ionizing particles at MeV energies [6], CsI(Tl) is a priori a good candidate, even better than NaI(Tl), for WIMP search which takes place at keV energies. However, no data were available at low energies, so we took advantage of the previous quenching factor measurements to digitize and record all selected nuclear recoil pulses. In the same experimental conditions were also accumulated low energy pulses of Compton interactions from a ^{137}Cs source. All pulses were digitized by a 200 MHz transient recorder for 4.2 μs, which represents about 4 times the characteristic scintillation decay time constant of CsI(Tl). To parametrise each pulse shape, we calculated for each event the first moment of the pulse height profile distribution,

$$t_m = \frac{\sum_i t_i \phi_i}{\sum_i \phi_i}, \qquad (5)$$

where ϕ_i is the amplitude of the pulse for each time channel t_i up to 4.2 μs.

On Fig. 4a and b the t_m values are plotted as a function of energy, respectively, for recoil and Compton events. Two clouds are observed with typical $\langle t_m \rangle$ values of 700 ns for recoils and of 1000 ns for Compton

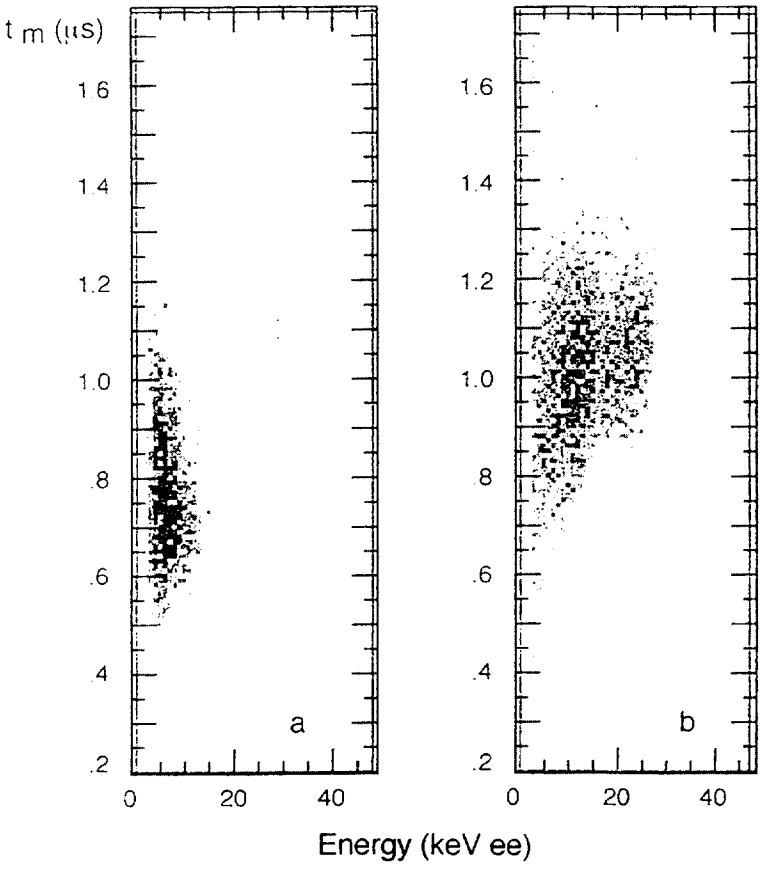

Fig. 4. t_m vs energy for (a) recoils and (b) Compton interactions.

events. The mean $\langle t_m \rangle$ values per 2 keV energy slice are shown on Fig. 5.

The quality of the separation depends also on the width of the t_m distributions per energy slice. This is taken into account in the quality factor Q, already used by CDMS [16] and EDELWEISS [17] groups, defined as

$$Q = \frac{\beta(1-\beta)}{(\alpha-\beta)^2}, \tag{6}$$

where $\alpha(\beta)$ are respectively the fraction of recoil (electron) events kept below a given value of the discrimination parameter, here t_m, for a given energy slice. The lower the Q, the better is the rejection power. so for each energy bin, the t_m selected value is chosen to minimize the Q factor. This Q value is shown as a function of the electron equivalent energy on Fig. 6, together with the values for NaI(Tl) [18].

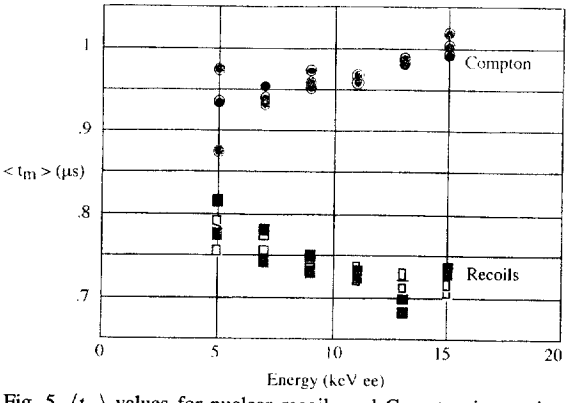

Fig. 5. $\langle t_m \rangle$ values for nuclear recoils and Compton interactions.

The CsI(Tl) appears definitely better than NaI(Tl) at the same electron equivalent energy, but this improvement is even higher at the same kinetic energy

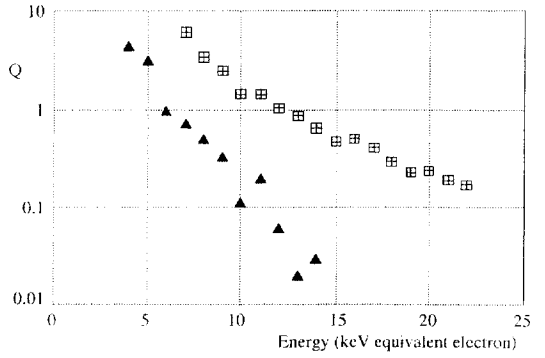

Fig. 6. Quality factor of CsI(Tl) (this study, triangles) and NaI(Tl) (squares, [18]).

because of the lower quenching factor of NAI(Tl) relative to CsI(Tl). For example, a 50 keV iodine recoil gives an equivalent electron energy of 4 keV in NaI(Tl) (quenching factor of 8%), while in CsI(Tl), it translates in 5.5 keV (quenching factor of 11%), with a Q factor higher than at 4 keV. This difference grows towards lower energies. Nevertheless, potential difficulties may arise from the higher PMT noise level at low energies in low counting rate environments for two reasons:

- the intrinsic noise of green extended photo-cathode is higher than the standard one used for NaI(Tl),
- the time constant of CsI(Tl) (at least 700 ns) is higher than the decay time of NaI(Tl), so there is a higher probability of getting random noise from the PMT in the time window defining a scintillation pulse.

5. Conclusion

The CsI(Tl) scintillator appears to be a good candidate for direct detection of WIMPs. Its luminous efficiency with a green extended photo-cathode photomultiplier is as high as the NaI(Tl) efficiency, and its quenching factor is higher by a factor of 2 at very low recoil energies. The amplitude and the increase of the quenching factor with decreasing energy are very well reproduced by the Birks model with Lindhard corrections for the nuclear part, with no threshold effect. Radioactive background rejection by using Pulse Shape Discrimination is also better. Another advantage of CsI(Tl) is its weak hygroscopic behaviour.

Building a low counting rate CsI(Tl) detector raises the problem of its internal radioactivity (137 and 134 Cs isotopes). To obtain CsI powders free from cesium isotopes for WIMP search, primary materials should be extracted from deep underground mines. Then handling powders and growing crystals requires special care to avoid ^{137}Cs environmental contamination. Actually, activity measurements of CsI powders with Germanium detectors at Laboratoire Souterrain de Modane have shown qualities not far from NaI powders ones.

References

[1] E. Gaillard-Lecanu, Thèse de l'Université Paris-XI-DAPNIA/SPP 94-20 (1994).
[2] A. Incicchitti, Int. Workshop at Tor. Vergata Univ. (June 1995).
[3] C. Bacci et al., Astropart. Phys. 2 (1994) 117.
[4] M.L. Sarsa et al., Proc. Int. Workshop TAUP95, Toledo (Sept. 1995).
[5] Osaka-Tokushima Collaboration, Proc. Int. Workshop TAUP95, Toledo (Sept. 1995).
[6] F. Benrachi et al., Nucl. Ins. Meth. Phys. Res. A 281 (1989) 137.
[7] G.J. Davies et al., Phys. Lett. B 322 (1994) 159.
[8] R. Gwin, R.B. Murray, I.R.E. Trans. Nucl. Sci NS-9 3 (1962) 28.
[9] J.B. Birks, Theory and Practice of Scintillation Counting (Pergamon, Oxford, 1964).
[10] J.P. Biersack, L.G. Haggmark, N.I.M. 174 (1980) 257.
[11] J. Lindhard et al., Mat. Fys. Medd. Dan. Vid. Selsk. 14 (1963).
[12] S. Bashkin et al., Phys. Rev. 109 (1958) 434.
[13] C. Pastor et al., N.I.M. 212 (1983) 209.
[14] B. Chambon, IPN-Lyon Internal Report (1998), to be published.
[15] D.J. Ficenec et al., Phys. Rev. D 36 (1987) 311.
[16] R.J. Gaitskell et al., The statistics of background rejection in direct detection experiment for dark matter, Nucl. Phys. B (Proc. Suppl.) 51B (1996) 279–283.
[17] D. Lhôte et al., Proc. Seventh Int. Workshop on Low Temperature Detectors (München) (27 July–2 August 1997) pp. 237–239.
[18] G. Gerbier et al., Astropart. Phys. 11 (1999) 287.